Journal of Materials Chemistry A

Accepted Manuscript

ROYAL SOCIETY OF CHEMISTRY

www.rsc.org/materialsA

Journal Name

ARTICLE

Synthesis and Characterization of the First Transparent Silicon Oxycarbide Aerogel Obtained Through H_2 Decarbonization

Received 00th January 20xx,
Accepted 00th January 20xx

DOI: 10.1039/x0xx00000x

www.rsc.org/

Sandra Dirè,[a, §] Evgeny Borovin[a], Masaki Narisawa[b] and Gian Domenico Sorarù[a, §]

Ambient dried aerogels (ambigels) have been synthesized from bis(triethoxysilyl)methane, BTEM and bis(triethoxysilyl)ethane, BTEE. The ambigels have been pyrolyzed at 800 and 1100 °C in flowing H_2 to obtain the corresponding SiOC aerogels. H_2 gas reacts with the organic moieties of the gel forming methane, which is eliminated in the gas phase and reduces the formation of the "free carbon" phase. The microstructural features of the SiOC aerogels have been characterized by N_2 sorption analysis while the molecular structure of the SiOC has been studied with multinuclear solid state NMR (^{29}Si, ^{1}H, ^{13}C) and FT-IR. When the BTEM ambigel is pyrolyzed in H_2 flow at 800 °C the decarbonization process is highly efficient and a bulk, transparent and *colorless* SiOC aerogel is obtained for the first time. The formation of the silicon oxycarbide network was verified by NMR and FT-IR study.

1. Introduction

Pyrolysis of polysiloxane precursors in inert atmosphere (Ar, He, N_2 or vacuum) usually leads to black shiny materials consisting of Si, O, and C, which are called "black glasses" [1]. These glasses have been discovered in the mid 80's and were proposed for high temperature structural applications [2-3]. The black color is believed to derive from the presence, in the amorphous network, of stacks of sp^2 C planes forming turbostratic or nanocrystalline graphite, also referred in the literature as "free C" or "excess C" phase [1]. The proper selection of the molecular structure and chemical composition of the starting precursor allows synthesizing silicon oxycarbide glasses with a minimum amount of free carbon [4]. Accordingly, transparent yellow-brown discs 5-6 mm in diameter and 500-800 μm thick have been obtained starting from hybrid sol-gel-derived precursors [5]. These SiOCs with minimum amount of free C display high quantum efficiency photoluminescence, PL, [6-7] in the visible region of the spectrum and can be easily doped with extra elements such as B [8] or even rare earth elements, Eu [9] or Er [10].

Recently, a new processing strategy to prepare SiOC glasses as white powders with minimum amount of extra carbon has been reported in the literature by the Narisawa group at Osaka Prefecture University [11]. According to this method the preceramic methyl-siloxane resin is treated in pure H_2 atmosphere at temperatures between 700 and 1300 °C. H_2 reacts with the organic side groups forming methane which is eliminated in the gas phase and reduces the excess carbon. The PL of these white SiOC materials obtained via the decarbonization process in H_2 gas has been thoroughly characterized and short-lived –at ca 410-500 nm - and long-lived – at 560 – 580 nm- photoluminescence has been reported [12].

From a processing point of view, in order to remove the free C, which forms in the silicon oxycarbide structure during pyrolysis, H_2 gas has to diffuse inward into the forming SiOC particles and CH_4 has to diffuse outward. If the diffusion path is too long then the process is not completely efficient, residual free carbon is left in the structure and the samples become yellow-brown-black depending on the amount of extra carbon. This is the reason why the decarbonization process is very efficient, leading to the production of white SiOC material, only on small methyl silsesquioxane particles (diameter ≤6 μm) [13]. Another type of samples for which the decarbonization process could be successfully applied should be precursors with a high level of interconnected open porosity. For these materials the flowing H_2 should easily permeate the entire sample through the open porous channels yet the diffusion path inside the solid material can still be very short and limited to the thickness of the solid network. Accordingly, to prove this idea, in this work we studied the formation of silicon oxycarbide glasses starting from highly porous sol-gel derived precursors, which are pyrolyzed in pure hydrogen atmosphere. We will show that the decarbonization process is indeed very efficient for these types of precursors and, for the first time, bulk transparent and *colorless* silicon oxycarbide glasses have been produced.

[a] *Dept. of Industrial Engineering, University of Trento, via Sommarive 9, 38123 Trento, Italy.*
[b] *Graduate School of Engineering Osaka Prefecture University, 1-1 Gakuen-Cho, Naka-Ku, Sakai, Osaka 599-8531, Japan.*
§ Corresponding Authors: Sandra Dirè, dire@ing.unitn.it
Gian Domenico Sorarù. soraru@ing.unitn.it

Electronic Supplementary Information (ESI) available: [details of any supplementary information available should be included here]. See DOI: 10.1039/x0xx00000x

2. Experimental

2.1 Sol-gel synthesis of the precursor

Ambient dried aerogels, also called ambigels, were prepared using two alkylene-bridged silicon alkoxides: bis(triethoxysilyl)methane, BTEM and bis(triethoxysilyl)ethane, BTEE. The silicon alkoxides were purchased from Aldrich Chemicals and were used without any further purification. A two step, acid/basic sol gel process was selected. The silicon alkoxides were dissolved in isopropanol and hydrolyzed with acidic water (3 mol L^{-1} $HCl_{(aq)}$) stirring for 1 h and then condensation was induced by adding drop wise an ammonia solution (13.36 mol L^{-1} $NH_{3(aq)}$). The molar ratio between Si alkoxides/isopropanol/$HCl_{(aq)}$/$NH_{3(aq)}$ was 1/5/4/4. (Isopropanol as a solvent has been selected since it has a low surface tension which reduces the capillary pressure resulting in high surface area ambigels [14]). After basic water addition the solutions were stirred for additional 5 min, the beakers were sealed with parafilm and kept at 50 °C . Gelation occurred within 2 h. The alcogels were aged for one week at 50 °C in closed environment, and then were solvent exchanged with isopropanol (3 times in 24 h) maintaining the gels at 50 °C. Final drying was accomplished very slowly (typically over 3 weeks) keeping the gels at 50 °C.

2.2 Pyrolysis process

Centimeter-sized ambigel samples were pyrolyzed in H_2 flow (ca 500 mL/min) up to 800 and 1100 °C with 1 h holding time at the maximum temperature. Based on previous experience [12], the samples were heated up to 600 °C at a rate of 300 °C/h maintained for 1 h at 600 °C and then heated at 200 °C/h up to the selected maximum temperature. The mass of the samples has been measured before and after pyrolysis in order to evaluate the weight loss during the process.

2.3 Microstructural characterization.

N_2 sorption experiments were carried out at 77 K on an ASAP 2010 Micromeritics instrument. The pyrolyzed samples were degassed below 1.3 Pa at 250 °C. The specific surface area (SSA_{BET}) was calculated by the BET equation in the interval $0.05 \le p/p_0 \le 0.33$ with a least squares fit of 0.998 giving an accuracy of ±10 m^2/g [15]. Single point total pore volume (TPV) was calculated at p/p_0 = 0.995. Pore size distribution was obtained from the adsorption branch of the isotherms using the BJH model [16]. The morphological features of the SiCO aerogels were analyzed from fresh fracture surfaces using a Supra 40 Zeiss field emission scanning electron microscope, FE-SEM, after Au film deposition by sputtering.

2.4 Structural characterization.

The structure of the resulting SiCO samples was characterized using FT-IR and multinuclear MAS NMR spectroscopies.

The FT-IR spectra were recorded in transmission mode using KBr pellets with a Thermo Optics Avatar 330 instrument in the 4000 – 400 cm^{-1} interval acquiring 64 scan and with 4 cm^{-1} resolution.

The solid state NMR analyses were carried out with a Bruker 400 WB spectrometer operating at a proton frequency of 400.13 MHz. Samples were packed in 4 mm zirconia rotors and spun at 7 kHz. ^{29}Si MAS NMR spectra were acquired at 79.49 MHz with SP and CP pulse sequences under the following conditions: π/4 pulse length: 2µs, recycle delay: 100s, 1k scans; contact time: 5ms, proton decoupling length 6.5 µs, 3k scans. Q_8M_8 was used as external secondary reference. The Si units are labeled according to the usual NMR notation : Q^n, T^n, D, M and X represent SiO_4, $SiCO_3$, SiC_2O_2, SiC_3O and SiC_4 units, respectively, and n is the number of oxo-bridges; T^H and D^H represent $HSiO_3$ and $HSiCO_2$, respectively. ^{13}C CPMAS spectra were recorded at 100.29 MHz, with π/4 pulse length 2.9µs, contact time 2 ms, proton decoupling length 3.7 µs, recycle delay 5s, 10k scans. ^1H SP sequence, was based on π/4 pulse length 5 µs, recycle delay 5s, 8 scans. Adamantane and EtOH were used as external secondary references.

2.4 Reflectance measurements

Reflectance measurements on powders were performed by illuminating the samples with an Ocean Optics reflection probe constituted by 6 silica fibers (600 µm diameter) for the light output around a central fiber for the collection of the reflected light. The light source was an Avantes-2000 deuterium-halogen lamp and the reflected spectrum was recorder with a FL-QE65000 Ocean Optics spectrometer. Before every spectrum the dark signal was collected by closing the lamp shutter and the white reference was obtained from a barium sulphate powder sample.

The measured reflectance was converted into Kubelka-Munk units with the formula:

$$\frac{K}{S} = \frac{(1-R)^2}{2R}$$

3. Experimental Results

Residual mass values of the studied samples after pyrolysis at 800 and 1100 °C are reported in **Table 1**.

Monolithic, crack-free and transparent ambigels have been obtained from both the starting alkoxides (**Figure 1**).

Pyrolysis in H_2 flow at 800 °C leads to a transparent and *colorless* material for the BTEM system while for the BTEE precursor the product is still mostly transparent but with an amber color. When the pyrolysis temperature is increased up to 1100 °C the BTEE-derived ceramic turns dark-brown and opaque while the BTEM leads to a pale-brown ceramics which is still transparent in some parts. These are quite remarkable results since it has never been reported before the formation, at 800 °C, of a transparent and *colorless* centimeter-sized bulk ceramic from the pyrolysis of a siloxane precursor. In general, starting from commercial methyl-substitute siloxane networks pyrolyzed in Ar flow, the transparency can be maintained up to ca 500°C and above that temperature the

samples become brown and opaque-black above 700 °C. Only using Si-H-containing precursor the transparency can be maintained up to 1000 °C but already at 500 °C the samples turn yellow-brown [5].

Table 1. Residual mass measured on the ambigels as a result of the pyrolysis in H_2 atmosphere and their appearance.

Sample	Residual Mass (%)	Appearence
BTEM 800 °C	67,7	Transparent and colorless with small cracks
BTEM 1100 °C	67,5	Pale – brown, transparent in some parts
BTEE 800 °C	67,8	Brown – yellow More transparent at the surface
BTEE 1100 °C	65,8	Dark – brown, opaque

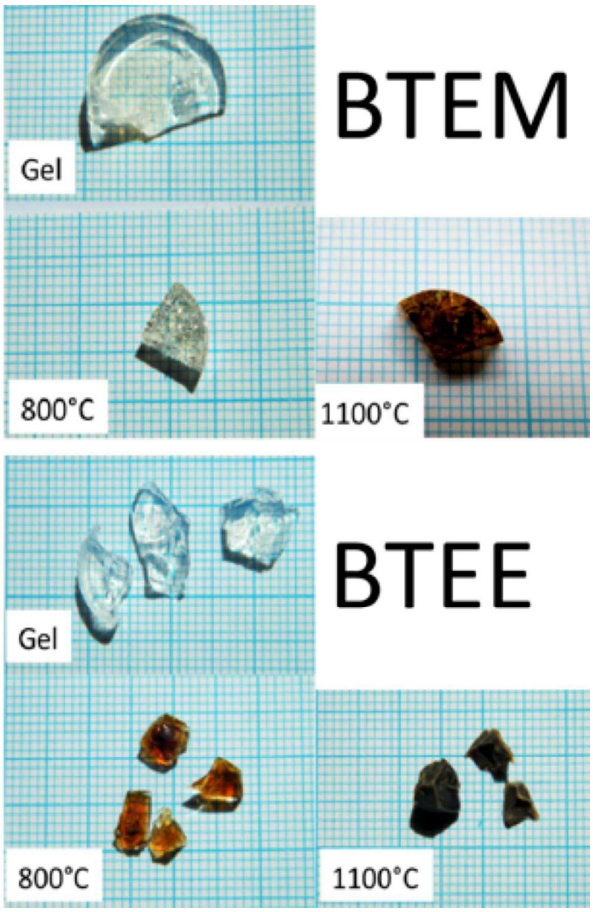

Figure 1. Optical micrographs of the starting aerogels and of the pyrolyzed materials.

Since the samples have irregular shape and cracks they are not amenable for classical transmittance measurements. Accordingly, the absorption in the visible range of the pyrolyzed samples was evaluated through total reflectance measurements and calculating the absorption spectra using Kubelka Munk units. In **Figure 2a** are shown the reflectance spectra of BTEM 800 and BTEE 800 samples. As can be observed sample BTEE 800 exhibits an average reflectance value considerably lower than BTEM 800 (55% against 78%) at wavelengths higher than 600 nm. At lower wavelengths the reflectance of BTEE 800 decreases, reaching around 20% at 400 nm, while the reflectance of BTEM 800 is still 67% at that wavelength. In **Figure 2b** the absorption spectra in Kubelka Munk units are reported. As can be observed, BTEM is characterized by a negligible absorption level in the visible range demonstrating that the material is intrinsically transparent. On the other hand, BTEE 800 absorbance slowly starts to increase at 600 nm and then gives an intense absorption peak in the UV region, at 228 nm, with a shoulder at 278 nm. This result indicates that in BTEE 800 glass matrix are present absorbing centers probably due to isolated carbon clusters.

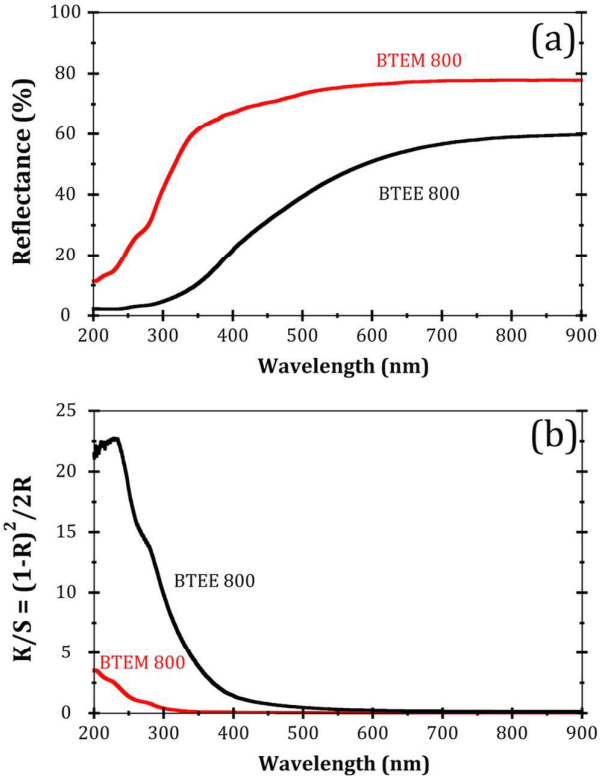

Figure 2. (a) total reflectance spectra and (b) absorption spectra in Kubelka Munk units for the BTEM and BTEE samples pyrolyzed at 800 °C.

3.1 N_2 sorption and FE-SEM characterization

N_2 sorption technique was applied to study the microstructure of the porous samples. The starting ambigels display high surface area around 1100 m^2/g, high pore volume - 0,80 and 1,29 cc/g for the BTEM and BTEE samples respectively - and narrow pore size distribution in the range 3 to 5 nm [14]. After pyrolysis treatment in pure H_2 gas the measured N_2 adsorption/desorption isotherms suggest that the mesoporous character of the material is maintained at both pyrolysis temperature. Indeed, for both systems and both temperatures the isotherms, which are shown in **Figure 3**, can be classified as Type IV with a hysteresis loop caused by the capillary

condensation in the mesopores regime (2–50 nm). Moreover, the isotherms present a steep rise of the adsorbed volume for $P/P_0<0.05$ indicating the presence of microporosity in the samples. The measured values of SSA_{BET} and TPV are reported in **Table 2.** At 800 °C high values of specific surface area, in the range 500-600 m^2/g and significant total porosity volume values, in the range 0.25 – 0.55 cm^3/g, have been measured for both samples. When the pyrolysis temperature is increased up to 1100 °C a slight reduction of SSA_{BET} and TPV is observed, however the samples still display high porosity.

The bulk density of the SiCO has not been measured since the samples had irregular geometry and cracks. However, from the total pore volume measured by N_2 adsorption and assuming a skeleton density value of ca 2 g/cm^3 for both SiCO compositions [17, 18], the bulk density for the samples pyrolyzed at 800 °c is estimated to be 1.3 and 0.9 g/cm^3 for the BTEM and BTEE samples respectively.

The cumulative pore volume as a function of the pore size for the two investigated aerogels is reported in **Figure 4.**

For both samples all the porosity is in the pore size range 20 – 100 Å. Interestingly, increasing the pyrolysis temperature from 800 to 1100 °C leads to a reduction of total porosity without a clear shift to lower dimension of the maximum pore size, which remains close to 100 Å.

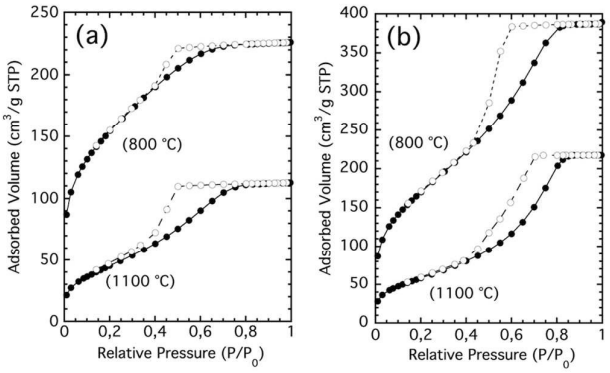

Figure 3. Adsorption/desorption isotherms recorded on the: (a) BTEM and (b) BTEE aerogels pyrolyzed under 100% H_2 flow.

Table 2. Specific surface area, SSA_{BET}, total pore volume, V_{total} and average pore size of the studied SiOC aerogels.

Sample	SSA_{BET} (m^2/g)	TPV (cm^3/g)	Pore size (Å)
BTEM-800 °C	536	0.25	19
BTEM-1100 °C	171	0.18	42
BTEE-800	615	0.58	38
BTEE-1100°C	217	0.34	63

The main effect of increasing the pyrolysis temperature seems a consumption of the smaller pores (Figure 4). To properly highlight this aspect the pore size distribution, PSD, curves have been evaluated (**Figure 5**). Indeed, PSD curves show a narrow pore size distribution with peak values, at 800°C, of 20-30 Å for the BTEM and 50 – 60 Å for the BTEE system. For both samples increasing the pyrolysis temperature from 800 to 1100°C leads to a slight shift of the peak toward higher pore sizes without changing the narrow pore size distribution. The shift to higher pore size is due to the relative decrease of the volume of the smaller micro and mesopores, which are known to vanish when the pyrolysis temperature is increased above to 800 – 900°C [19, 20, 21].

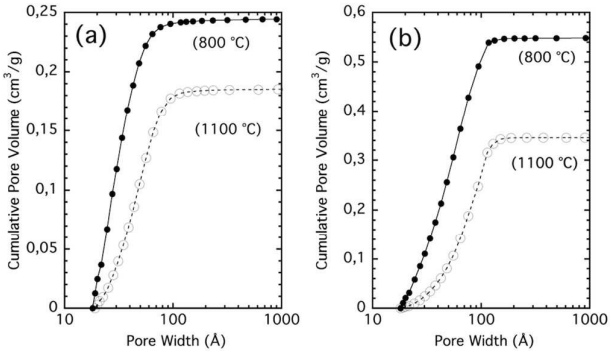

Figure 4. Cumulative pore volume as a function of the pore size obtained from the adsorption branch of the isotherms for the two studied aerogels pyrolyzed in H_2 flow at 800 and 1100 °C. (a) BTEM and (b) BTEE system

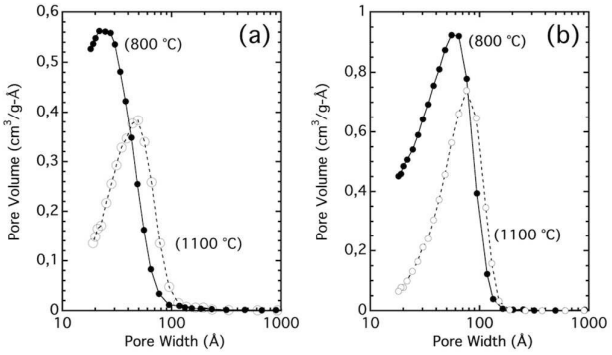

Figure 5. Pore size distribution curves obtained from the adsorption branch of the isotherms for the: (a) BTEM and (b) BTEE aerogels pyrolyzed under 100% H_2 flow.

The porous features of the SiCO samples of both compositions has been also confirmed with the FE-SEM study of the fracture surfaces. The FE-SEM investigation revealed rough fracture surfaces typical of mesoporous materials (**Fig. S1**). BTEE samples display a rougher surface compared to the BTEM one in agreement with the larger pore size revealed by the N_2 adsorption analysis.

3.2 MAS NMR Characterization

^{29}Si MAS NMR is the best tool in order to assess the formation of the silicon oxycarbide network in which silicon atoms bond at the same time oxygen and carbon atoms forming mixed silicon oxycarbide units [22, 23, 24].

The ^{29}Si SPMAS spectra recorded on the pyrolyzed samples are shown in **Figure 6** and are characterized by two main signals at -107 and between -70 and -65 ppm, due to SiO_4 (Q) and $SiCO_3$ (T) units respectively. The weak resonances detected between +5 and -40 ppm can be assigned to a combination of SiC_3O (M), SiC_4 (X) and SiC_2O_2 (D) units [23]. In the samples treated at 800 °C, D units present a resolved signal at -25 ppm, whereas the resonances of M and X units in the range +5 ÷ -10 ppm are very weak and almost negligible.

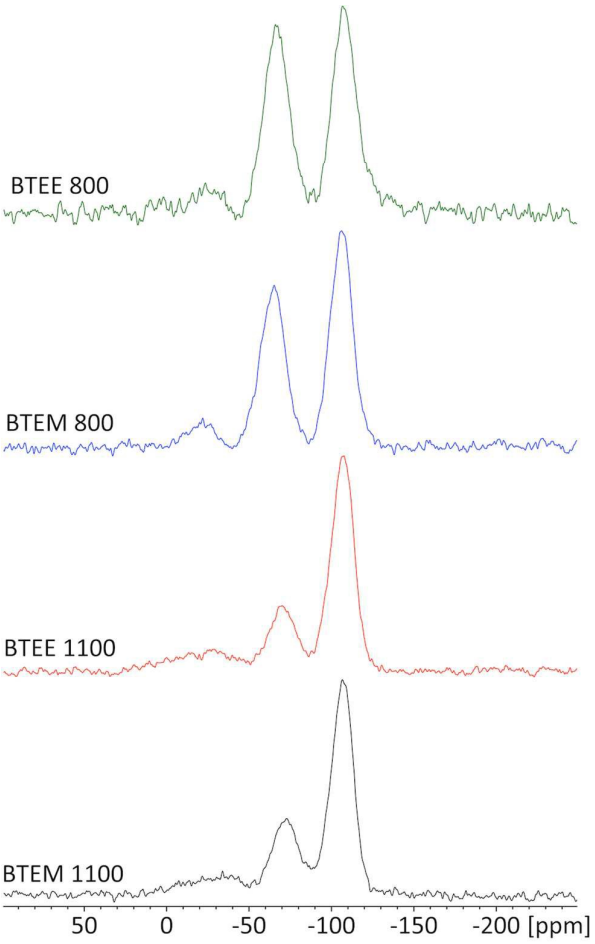

Figure 6. ^{29}Si SPMAS NMR spectra of the SiOC aerogels pyrolyzed in 100% H_2 flow at 800 and 1100 °C.

Increasing the temperature from 800 to 1100 °C results into a decrease in intensity and a shift towards high fields of T peaks. In particular, the resonance of T units moves from -65 ppm at 800°C to -72 ppm at 1100°C. The upfield shift of D units from -25 to -35 ppm is also observed at 1100 °C.

The results of the profile fitting analysis of the SPMAS spectra are shown in **Table 3**.

Table 3. Quantitative results calculated from ^{29}Si SPMAS spectra. (Confidence level 96%)

Si units	BTEM 800, %	BTEM 1100, %	BTEE 800, %	BTEE 1100, %
SiO_4	54.1	63.0	48.1	61.7
$SiCO_3$	38.1	25.2	38.7	19.0
SiC_2O_2	6.4	9.6	10.2	8.1
SiC_4, SiC_3O	1.4	2.2	3.0	11.2

Increasing the temperature from 800 to 1100 °C leads to a decrease of the amount of $SiCO_3$ (T) units and a corresponding increase of the SiO_4 (Q). An increase of the total amount of the C-rich mixed silicon units, SiC_xO_{4-x}, x = 2,3,4 (SiC_2O_2 (D), SiC_3O (M) and SiC_4 (X) units) is also observed from 800 to 1100 °C. This evolution of the local environment of the silicon atom with the pyrolysis temperature is due to the occurrence of redistribution reactions between Si-O and Si-C bonds, as was clearly show by Mutin [25].

It has been shown by Tavakoli et al. that pyrolysis in H_2 flow of a methylsiloxane resin leads to the production of SiOC materials with a high residual hydrogen content which is mainly present in the structure as C-H bonds. [26]. Therefore, ^{29}Si CPMAS experiments, taking advantage from the magnetization transfer in proton-rich environments, could bring more information on the silicon sites, in particular those which are in close proximity with the residual hydrogen atoms. **Figure 7** shows the ^{29}Si CPMAS spectra of BTEM and BTEE samples treated at 800 and 1100 °C. The signal-to-noise ratio indicates that the efficiency of magnetization transfer benefits from a fair amount of bonded hydrogen even at 1100 °C.

Contrary to the SPMAS NMR spectra, the most intense signal is the one at -65 ppm due to T units suggesting that the carbon atoms of the $SiCO_3$ sites may often be present as CH_x (x = 1, 2) groups. For the same reason the component due to D units is enhanced compared to the SPMAS NMR spectra and appear now as a well resolved peak. The signals due to X and M units can be clearly detected only at 1100 °C. Increasing the temperature from 800 to 1100 °C does not substantially modify the NMR spectra –only a small relative decrease of the intensity of the T units component compared to the Q and D peaks can be observed- suggesting that H bonded to carbon atoms of the mixed silicon units is present in significant amount in the SiOC structure up to this temperature. This result is in agreement with the high amount of H (4.4 at%) found in a methylsiloxane resin pyrolyzed in H_2 flow at 1100°C [26]. At 800 °C, the good signal-to-noise ratio of the spectra allows to clearly identify an up-field shoulder in the peak of the T units. In order to precisely measure the chemical shift of the Si sites giving rise to this shoulder a fitting of the 800 °C spectra has been performed. The results, shown in **Figure 8**, indicate that, not only the T peak at -65 ppm has an extra up-field component at -83 ppm

but also the resonance at -24 ppm (D units) has an up-field component at -35 ppm. The two new peaks at – 35 and – 83 ppm

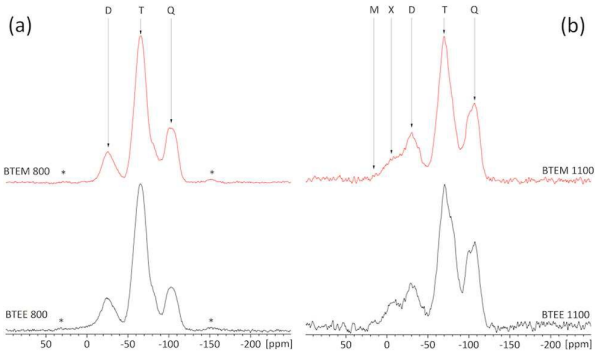

Figure 7. ^{29}Si CPMAS spectra of the samples treated at 800 (a) and 1100 °C (c). (The spinning sidebands are marked with *)

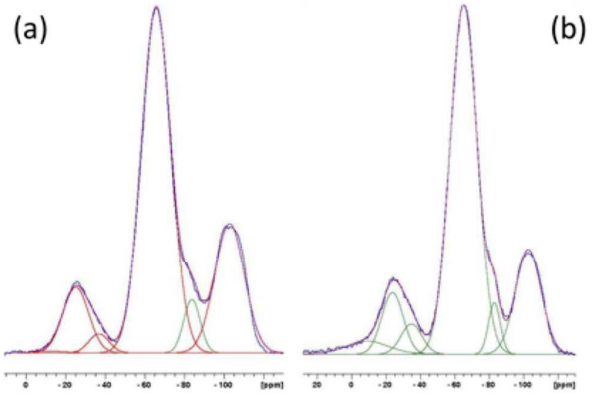

Figure 8. Experimental and simulated ^{29}Si CPMAS spectra of the samples pyrolyzed at 800 °C. (a) BTEM and (b) BTEE precursors.

can be assigned to D^H and T^H [27] sites respectively and reveal the presence of hydrogen bonded directly to silicon atoms forming Si-H bonds. The presence of Si-H bonds in the pyrolysis product of a methylpolysiloxane resin was already reported, based on FT-IR studies, for materials pyrolyzed in Ar atmosphere at temperature between 800 and 900 °C [18, 28] and more recently, for SiOCs pyrolyzed in H_2 flow, based on ^{1}H MAS NMR studies [26]. The presence of Si-H bonds in the SiOC aerogels will be confirmed by the ^{1}H MAS NMR and FT-IR studies that will be shown further on in this article.

Similar deconvolution of the ^{29}Si CPMAS NMR spectra of the 1100°C samples reveals the permanence of the two shouldes of the D and T peaks related to the Si-H bonds. Moreover, the peak assigned to the SiO_4 units splits into two components at around -100 and -108 ppm, assigned to Q^3 and Q^4 units, respectively. The Q^3 units, in which silicon is bonded to three bridging and one terminal oxygen indicates the presence of Si-OH groups.

The ^{1}H MAS NMR spectra of BTEE annealed at 800 and 1100 °C (**Figure 9**) are characterized by the main resonance centered at about 4.2 ppm that shows a small downfield shift and broadening with increasing the temperature. The signal can be attributed to protons in adsorbed water and silanols [23]. However the presence of protons directly linked to silicon cannot be excluded in agreement with the reported position of Si-H resonance at 4.1 ppm [26]. At 800 °C, different weak signals can de detected at around 0, 1.3 and 2.1 ppm leading, at 1100 °C, to the broad resonance centered at 1 ppm, related to protons linked to sp^3 carbon atoms in residual CH_x (x = 1, 2) sites [23]. The ^{1}H NMR spectra have been deconvoluted to get the quantitative amounts of the individual components. The principal peak has been simulated with two components, a broader one at 4.4 ppm and a narrow one at 4.1 ppm. The component at 4.4 ppm has been assigned to molecular water and Si-OH while the one at 4.1 ppm has been tentatively attributed to Si-H bonds. With this assumption, the relative amount of the Si-H and C-H bonds (bands in the range 0 – 2.2 ppm) can be estimated to be of the order of 46% to 26% respectively at 800 °C (the remaining up to 100% is attributed to H_2O and Si-OH) and for 20 % to 26% at 1100 °C.

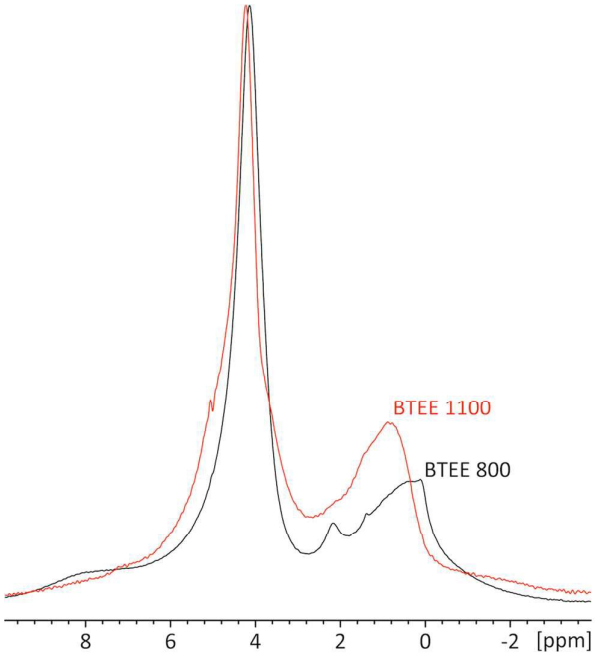

Figure 9. ^{1}H MAS NMR spectrum of BTEE 800 (black) and BTEE1100 (red).

The ^{29}Si and ^{1}H NMR study indicates that Si-H and C-H bonds are retained in the SiOC network up to 1100 °C. Indeed, a ^{13}C CPMAS spectrum recorded on BTEE1100 **(not shown),** despite the poor signal-to-noise ratio, displays a very broad signal at 6.8 ppm that can been assigned to a distribution of linked, sp^3 bonded $–CH_x$ sites with x ranging from 0 to 2 [29].

3.3 FT-IR Characterization

The FTIR spectra of the different samples are reported in **Figure 10**. The spectra display the intense bands of adsorbed water (3450 and 1630 cm^{-1}) in agreement with the high porosity of samples. The stretching vibration of hydrogen-bonded Si-OH groups can be detected at 3646 cm^{-1} as a shoulder of the main peak due to adsorbed molecular water. The Si-H stretching vibration is clearly identified at 2273 cm^{-1} in the spectra of samples pyrolyzed at 800 °C while it cannot be detected at higher temperature. The frequency range and the broadness of the Si-H bond stretching vibration suggest that the signals can be attributed to T^H units (2273 cm^{-1}) with some contribution of D^H (2200 cm^{-1}) units [27, 30, 31], in agreement with the previously presented NMR results.

At 800 °C the Si-O asymmetric stretching band presents the main signal at 1053 and 1062 cm^{-1} for BTEE and BTEM, respectively. The band shifts to 1083 cm^{-1} for both samples at 1100°C. The intensity and position of the high frequency shoulder on the siloxane band (at about 1190 cm^{-1}) changes in the different samples. Two well resolved signals at 880 and 800 cm^{-1} can be observed in samples annealed at 800 °C. At 1100 °C the signals broaden and the low frequency vibration moves to 820 cm^{-1}. The bands in the range 900-700 cm^{-1} are due to the overlapping of Si-O symmetric stretching (≈ 800 cm^{-1}), Si-CH_x with x = 0, 1, 2 (880-780 cm^{-1}) and O-Si-H bending vibrations (≈ 880 cm^{-1}).

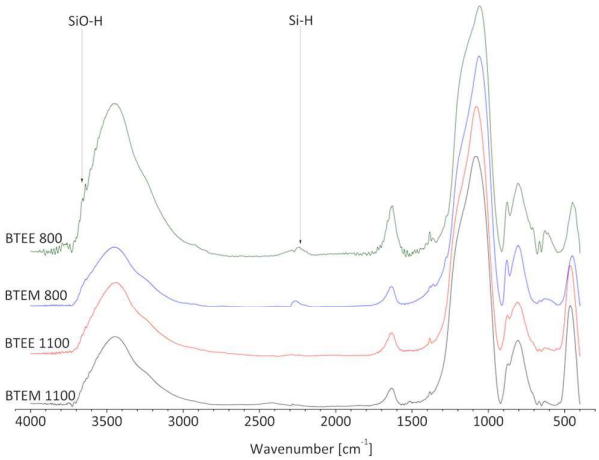

Figure 10. FTIR spectra of the SiOC aerogels pyrolyzed in H_2 flow at 800 and 1100°C.

4. Discussion

The synthesis of silicon oxycarbide glasses with negligible free carbon content has been previously reported by our group at the University of Trento starting from sol-gel-derived silicon alkoxides containing Si-CH_3 as well as Si-H groups. The relative amount of methyl and Si-H moieties which needs to be present in the starting gel in order to obtain, after pyrolysis, a stoichiometric silicon oxycarbide phase without extra carbon was estimated based on the assumption that the atomic O/Si ratio does not change during pyrolysis. With the same assumption and considering a fully condensed gel network the theoretical weight losses during the H_2 pyrolysis can be estimated according to the following reactions:

$$HC_{0.5}SiO_{1.5} + H_2 \rightarrow C_{0.25}SiO_{1.5} + 0.25CH_4 + H_2 \quad \frac{\Delta W}{W_0} = -6.8\% \quad (1)$$

$$H_2CSiO_{1.5} + H_2 \rightarrow C_{0.25}SiO_{1.5} + 0.75CH_4 + \frac{1}{2}H_2 \quad \frac{\Delta W}{W_0} = -16.6\% \quad (2)$$

where reaction (1) refers to the BTEM and reaction (2) to the BTEE system. The chemical formula of the BTEM and BTEE precursors have been calculated based on the following building blocks of the two fully condensed siloxane resins:

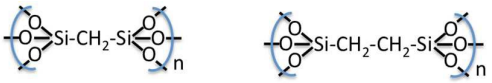

BTEM BTEE

The experimental weight losses (see Table 1) are in the range 32 – 34 %, i.e. higher than the estimated ones and independent from the studied system. Higher experimental weight losses during pyrolysis are probably related to the residual OH and ethoxy groups present in the starting siloxane network. Indeed, the pyrolysis in Ar flow of the same two precursors showed a weight loss step below 200 °C due to evolution of H_2O and decomposition of un-hydrolyzed Si-OEt moieties [14]. Interestingly the intensity of the weight loss step below 200°C reported in [14] is higher for the BTEM system compared to the BTEE one justifying why, in the present case, we observe similar weight losses for both gels.

Pyrolysis in H_2 flow at 800°C resulted into the formation of transparent and *colorless* bulk sample for the BTEM system while the BTEE one is still transparent in some parts but it has a pale–brown color. The absorption spectrum in Kubelka Munk units (see **Figure 2**) for the BTEM is characterized by a negligible absorption level in the visible range suggesting that the material is intrinsically transparent. This result is remarkable since it has never been reported before the synthesis of a silicon oxycarbide (in form of a bulk sample, not as powder or thin film) which is transparent and *colorless* after a pyrolysis process at temperature as high as 800°C. The pale-brown color showed by the SiOC material obtained from BTEE precursor suggests the presence of traces of free carbon in this sample. Indeed for this sample the absorbance slowly starts to increase at 600 nm and then gives an intense absorption peak in the UV region. Actually according to reaction (2) the amount of carbon that must be removed from the system as methane in order to obtain a stoichiometric network (without the formation of extra carbon phase) is three times the amount of carbon that has to be removed from the BTEM precursor. It is also worth of noticing that, according to reaction (1), BTEM precursor has enough hydrogen in its structure to form the stoichiometric amount of methane and the external H_2 flow provides excess reagent (H_2) to promote the kinetics while for the BTEE gel the H_2 supplied by the gas flow is required to fulfill the stoichiometry of the reaction. Taken all

together these observations explain why it is easier to produce a transparent and colorless SiOC from the BTEM precursor compared to the BTEE one.

To confirm the formation of the silicon oxycarbide network we run ^{29}Si SP MAS-NMR spectra and the results actually showed the fingerprint of the SiOC material (see **Figure 6**) with the presence of mixed SiC_xO_{4-x} $0 \leq x \leq 4$ units. At 800°C the ^{29}Si spectra of both compositions are dominated by the signals related to SiO_4 (Q) units at -107 ppm and $CSiO_3$ (T) units between -70 and -65 ppm. Increasing the pyrolysis temperature to 1100°C leads to a decrease of the T units which transform into Q and D, M and X units. Noticeably, from 800 to 1100°C the position of the T units shifts to high fields (from -65 to – 72 ppm) as a consequence of the dehydrogenation occurring in this temperature range with the transformation of some terminal C-H bonds into bridging C-Si bonds as already reported in the literature for a similar Si-O-C systems [33].

At 1100°C the relative amount of the different Si sites is in line with similar data reported in the literature for silicon oxycarbide glasses obtained from methyl substituted silica gels pyrolyzed in inert atmosphere at 1000 – 1100°C [14, 34]. This result shows that the pyrolysis in H_2 flow –as compared with the pyrolysis in Ar atmosphere- does not change the composition of the silicon oxycarbide network but the main difference between these two treatments is the amount of the free C phase which is very different in the two cases. Indeed, the transparent and colorless material obtained at 800 °C from the BTEM precursor suggests that the presence of free carbon in the oxycarbide structure is extremely low – if any - while for the same sample pyrolyzed in Ar flow 70% of the carbon atoms were present in the free carbon phase [14].

Another important difference between the SiOC materials produced in H_2 flow compared to those obtained in inert atmosphere such as Ar, is the H content which can go up o 4.4 at% [26]. In order to precisely identify the H chemical sites we performed complementary analysis including ^{29}Si CP-MAS NMR, ^{1}H MAS NMR, ^{13}C MAS NMR and FT-IR. Accordingly, the enhancement of T and D units in the ^{29}Si CPMAS NMR spectra compared to ^{29}Si SPMAS NMR spectra reveals the occurrence of $-CH_x$ $1 \leq x \leq 2$ moieties bonded to Si atoms. The same C-H bonds leads to the broad resonance at 6.8 ppm in the ^{13}C CPMAS NMR spectrum that can been assigned to a distribution of linked, sp^3 bonded $-CH_x$ sites with x ranging from 0 to 2.

Si-H bonds are also present in the silicon oxycarbide. They give rise to individual components at -35 and -83 ppm in the ^{29}Si CPMAS-NMR spectra as well as to absorptions at ca 2270 cm^{-1} in the FT-IR spectra. Interestingly, the ^{1}H MAS NMR analysis performed on the SiOC sample obtained from the BTEE precursor pyrolyzed at 800 and 1100 °C reveals that, the hydrogen is bonded not only to carbon, forming C-H bonds, but also to silicon, forming Si-H groups. At 1100°C the estimated (Si-H)/(C-H) molar ratio is roughly 1:1. Finally, hydrogen is present in the materials also as silanols, Si-OH, as clearly reveald by the: (i) ^{29}Si CPMAS NMR (presence of Q^3 Si sites) and FT-IR (absorption at 3646 cm^{-1}). Si-OH moieties are probably formed after pyrolysis through a room temperature reaction with laboratory atmosphere [28].

The formation of SiOC aerogels was confirmed by the N_2 sorption analysis (see Figg. 3,4,5 and Table. 1), which clearly reveals the highly mesoporous character of the samples at both pyrolysis temperatures. It is worth of noticing that the important porosity level is maintained up to a high pyrolysis temperature (1100 °C). Since the studied samples have, if any, minimal free carbon amount, the absence of an important sintering phenomena up 1100 °C –that would have lead to the complete disappearance of the mesopores - must be associated with the presence of Si-C bonds of the silicon oxycarbide network. This observation contributes to shed some light on the origin of the high viscosity shown by the polymer derived amorphous ceramics (SiCO and SiCN) which has been attributed, in some papers [35], to the presence of a the network of sp^2 C planes more than to the presence of tetracoordinated carbon atoms in the amorphous structure.
Finally, the combination, in just one material, of high temperature stability –as a result of the silicon oxycarbide network- and the better oxidation resistance provided by the absence of the free carbon phase with the high porosity and optical transparency could afford a new functional material different fields in harsh environment such as high temperature optical application, membranes or catalytic supports. We are currently testing these aerogels as optical sensors for different gases.

Conclusions

In this study, two ambient dried aerogels (ambigels) were synthesized from two different alkylene-bridged silicon alkoxides: bis(triethoxysilyl)methane, BTEM and bis(triethoxysilyl)ethane, BTEE. The ambigels have been pyrolyzed in pure H_2 flow at 800 and 1100°C to obtain the corresponding SiOC aerogels. The BTEM precursor pyrolyzed at 800°C leads to the formation of a bulk, transparent and colorless sample while for the BTEE system at the same temperature the material is still transparent but brown-yellow. The N_2 sorption analysis demonstrated that the pyrolyzed samples are higly porous with narrow pore size distribution around 20-30 Å and 50-60Å for the BTEM and BTEE systems respectively. The ^{29}Si MAS NMR clearly proved the formation of the silicon oxycarbide network for both samples at both temperatures. Taken all together these results suggest that after pyrolysis in H_2 flow the starting ambigels lead to the formation of silicon oxycarbide aerogels. The BTEM composition pyrolyzed at 800 °C, leads to a silicon oxycarbide aerogel that is, for the first time, transparent and colorless, suggesting that the free carbon phase is present, if any, only in traces amount. The multinuclear ^{29}Si, ^{1}H and ^{13}C MAS NMR and FT-IR characterization revealed that hydrogen is still present in the materials up to 1100 °C as C-H, Si-H and Si-OH groups. ^{1}H

MAS NMR indicates that, contrary to what has been reported so far in the literature, H is not present mainly in C-H bonds but Si-H moieties are equally important. These new transparent, colorless and highly porous SiOC aerogels could lead to the discovery of a new class of optical materials with potential application in the field of optical sensors to be used also in aggressive environments.

Acknowledgements

This work was performed in the frame of the European COST action MP1202 "Rational design of hybrid organic-inorganic interfaces: the next step towards advanced functional materials".

Dr. Emanuela Callone ("Klaus Müller NMR Laboratory", University of Trento) is warmly acknowledged for the NMR spectra collection. The contribution of Dr. P.R. Aravind in the ambigels preparation is gratefully acknowledged.

Prof. Alberto Quaranta from the University of Trento is sincerely acknowledged for the reflectance measurements and their discussion.

References

1 C. G. Pantano, A. K. Singh and H. Zhang, *J. Sol Gel Sci. Technol.,* 1999, **14**, 7.
2 F.K. Chi, *Ceram. Eng. Sci. Proc.,* 1983, **4**, 704.
3 G.M. Renlund, S. Prochazka, and R.H. Doremus, *J. Mater. Res.*, 1991, **6**, 2716.
4 G. D. Sorarù, *J. Sol-Gel Sci. Technol.,* 1994, **2**, 843.
5 A. Quaranta, A. Karakuscu and G. D. Soraru, "Optical Properties." in *Polymer Derived Ceramics*, by P. Colombo, R. Riedel, G.D. Sorarù and A. Kleebe, p-253-261. Lancaster, PA: DEStech Publications (2009).
6 S. Gallis, V. Nikas, H. Suhag, M. Huang and A. E. Kaloyeros, *App. Phys. Lett.,* 2010, **97**, 081905, doi:10.1063/1.3482938.
7 A. Karakuscu, R. Guider, L. Pavesi and G. D. Sorarù, *J. Am. Ceram. Soc,* 2009, **92**, 2969.
8 A. Karakuscu, R. Guider, L. Pavesi and G. D. Sorarù, *Thin Solid Films,* 2011, **519**, 3822.
9 Y. Zhang, A. Quaranta and G. D. Soraru, *Optical Materials,* 2004, **24**, 601.
10 G. D. Sorarù, Y. Zhang, M. Ferrari, L. Zampedri and R. R. Goncalves, *J. Europ. Ceram. Soc.,* 2005, **25**, 277.
11 M. Narisawa, S. Watase, K. Matsukawa, T. Dohmaru, *Bull. Chem. Soc. Jpn.,* 2012, **85**, 724.
12 M. Narisawa, T. Kawai, S. Watase, K. Matsukawa, T. Dohmaru, K. Okamura and A. Iwase, *J. Am. Ceam. Soc.,* 2012, **95**, 3935.
13 M. Narisawa, A. Iwase, S. Watase, K. Matsukawa′ and T. Kawai, *Ceram. Transactions,* 2014, **243**, 79.
14 P. R. Aravind and G. D. Soraru, *Microp. Mesop. Mater.,* 2011, **142**, 511.
15 S. Brunauer, P.H. Emmet and E. Teller, *J. Am. Chem. Soc.,* 1938, **60**, 309.
16 E.P. Barrett, L.G. Joyner and P.P. Halenda, *J. Am. Chem. Soc.,* 1951, **73**, 373.
17 G. D. Sorarù, E. Dallapiccola, G. D'Andrea, *J.Am. Ceram. Soc.,* 1966 **79**, 2074.
18. L. Bois, J. Maquet, F. Babonneau, H. Mutin and D. Bahloul, *Chem. Mater.,* 1994, **6**, 796.
19. Y. Blum, G. D. Sorarù, A. P. Ramaswamy, D. Hui, and S. M. Carturan, *J. Am. Ceram. Soc.,* 2013, **96**, 2785.
20 J. Wan, M. J. Gasch and A. K. Mukherjee, *J. Am. Ceram. Soc.,* 2001, **84**, 2165.
21 H. Schmidt, D. Koch, G. Grathwohl, and P. Colombo, *J. Am. Ceramic Soc.,* 2001, **84**, 2252.
22 F. Babonneau, G. D. Soraru, G. D'Andrea, S. Dirè and L. Bois, *Mat. Res. Soc. Symp. Proc.,* 1992, **271**, 789.
23 H. Bréquel, J. Parmentier, S. Walter, R. Badheka, G. Trimmel, S. Masse, J. Latournerie, P. Dempsey, C. Turquat, A. Desmartin-Chomel, L. Le Neindre-Prum, U.A. Jayasooriya, D. Hourlier, H.-J. Kleebe, G. D. Sorarù, S. Enzo and F. Babonneau, *Chem. Mater,*. 2004, **16**, 2585.
24 S. J. Widgeon, S. Sen, G. Mera, E. Ionescu, R. Riedel and A. Navrotsky, *Chem. Mater.,* 2010, **22**, 6221.
25 H. P. Mutin, *J. Am. Ceram. Soc.,* 2002, **85**, 1185.
26 A. H. Tavakoli, M. M. Armentrout, M. Narisawa, S. Sen and A. Navrotsky, *J. Am. Ceram. Soc.,* 2015, **98**, 242.
27 G. D. Sorarù, G. D'Andrea, R. Campostrini and F. Babonneau, *J. Mater. Chem.,* 1995, **5**, 1363.
28 A. K. Singh and C. G. Pantano, *J. Sol-Gel Sci. Technol.,* 1997, **8**, 371.
29 B. Toury, F. Babonneau, *J. Europ. Ceram. Soc.,* 2005, **25**, 265.
30 G. D. Sorarù, R. Campostrini, S. Maurina and F. Babonneau, *J. Am. Ceram. Soc.,* 1997, **80**, 999.
31 M. Narisawa, T. Kawai, S. Watase, K. Matsukawa and A. Iwase, *AIP Advances,* 2014, **4**, 017118.
32 A. Grill and D. A. Neumayer, *J. Appl. PHys.,* 2003, **94**, 6697.
34 A. Pauletti, S. Handjani, C. Fernandez-Martin, C. Gervais and F. Babonneau, *J. Jap. Ceram. Soc.,* 2008, **116**, 449.
35 L. Bois, J. Maquet, F. Babonneau, H. Mutin and D. Bahloul, *Chem. Mater.*, 1994, **6**, 975.
36 A. Scarmi, G. D. Sorarù and R. Raj, *J. Non-Cryst. Solids,* 2005, **351**, 2238.

Journal Name

Entry For The Table Of Contents

Synthesis and Characterization of First Transparent Silicon Oxycarbide Aerogel Obtained Through H_2 Decarbonization

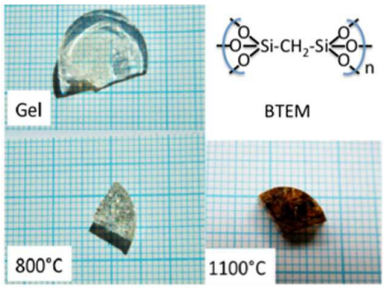

Sandra Dirè, Evgeny Borovin, Masaki Narisawa and Gian D. Sorarù

The first transparent silicon oxycarbide aerogel has been obtained through H_2 decarbonzation at 800°C starting from alkylen-bridged silicon alkoxide precursor.